Scaling flow diagram in the fractional quantum Hall regime of GaAs/$Al_xGa_{1-x}As$ heterostructures

S. S. Murzin,[1] S. I. Dorozhkin,[1] D. K. Maude,[2] and A. G. M. Jansen[3]
[1]*Institute of Solid State Physics RAS, 142432, Chernogolovka, Moscow District, Russia*
[2]*Grenoble High Magnetic Field Laboratory, Max-Planck-Institut für Festkörperforschung and Centre National de la Recherche Scientifique, Boîte Postale 166, F-38042, Grenoble Cedex 9, France*
[3]*Service de Physique Statistique, Magnétisme, et Supraconductivité, Département de Recherche Fondamentale sur la Matière Condensée, CEA-Grenoble, 38054 Grenoble Cedex 9, France*
(Received 7 September 2005; published 11 November 2005)

The temperature driven flow lines of the Hall and dissipative magnetoconductance data $(\sigma_{xy}, \sigma_{xx})$ are studied in the fractional quantum Hall regime for a two-dimensional (2D) electron system in GaAs/$Al_xGa_{1-x}As$ heterostructures. The flow lines are rather well-described by a recent unified scaling theory developed for both the integer and the fractional quantum Hall effect in a totally spin-polarized 2D electron system which predicts that one $(\sigma_{xy}, \sigma_{xx})$ point determines a complete flow line.

DOI: 10.1103/PhysRevB.72.195317 PACS number(s): 73.43.Fj, 72.25.Dc

The scaling treatment was initially proposed for the integer quantum Hall effect (QHE) using a graphical representation of the magnetoconductance data in the form of the flow diagram.[1–3] The flow diagram depicts the coupled evolution of the diagonal (σ_{xx}) and Hall (σ_{xy}) conductivity components due to diffusive interference effects. The similarity of many features at different integer and fractional quantum Hall states stimulated the creation of unified scaling theories.[4–8] The results of these theories are in qualitative agreement with each other, however, the phenomenological approach[4–7] provides a quantitative picture, the experimental verification of which is the goal of our investigation.

In Ref. 4, the conjecture was made that the scaling flow diagram for a totally spin-polarized electron system is invariant under the modular transformation

$$\tilde{\sigma} \leftrightarrow \frac{a\sigma + b}{2c\sigma + d}, \tag{1}$$

for complex conductivity $\sigma = \sigma_{xy} + i\sigma_{xx}$ where a, b, c, and d are integers with $ad - 2bc = 1$. This means that any part of the flow diagram in the $(\sigma_{xy}, \sigma_{xx})$ plane can be obtained from any other part by transformation (1) with corresponding choice of a,b,c, and d. Such transformations can be considered[6] as an extension of the "law of corresponding states" describing the symmetry relations between the different QHE phases.[9] For a holomorphic scaling β function in the variable $\sigma_{xy} + i\sigma_{xx}$ exact expressions for the flow lines have been derived.[5]

The structure of the theoretical flow diagram,[5] periodic along the σ_{xy} axis, is shown in Fig. 1 for one period $0 < \sigma_{xy} < 1$ (σ_{xx} and σ_{xy} are in units of e^2/h). For $\sigma_{xx} \gg 1$, the points $(\sigma_{xy}, \sigma_{xx})$ flow down vertically with increasing coherence length L, deviate from the vertical at about $\sigma_{xx} \sim 1$, and converge to integer values of σ_{xy} (0 or 1 for the range under consideration) on approaching the semicircle separatrix

$$\sigma_{xx}^2 + [\sigma_{xy} - 1/2]^2 = 1/4. \tag{2}$$

The points on the vertical separatrix $\sigma_{xy} = 1/2$, separating different QHE phases, flow vertically to the critical point $(1/2, 1/2)$ both from above and from below. Equation (1) maps the vertical separatrix at $\sigma_{xy} = 1/2$ into semicircle separatrixes connecting pairs of points $(p_i/q_i, 0)$ for odd integer p_i, and even integer q_i, with flow out from these points. The semicircle separatrix Eq. (2) is mapped onto semicircle separatrixes connecting pairs of points $(p_i/q_i, 0)$ with odd q_i and flow direction towards these points corresponding to either an integer $(q_i = 1)$ or fractional $(q_i > 1)$ quantum Hall state, or an insulating state $(p_i = 0)$. Crossings of the different type semicircle separatrixes produce the fixed critical points. All flow lines different from the separatrixes leave from the points $(p_i/q_i, 0)$ with even q_i and arrive at the points $(p_i/q_i, 0)$ with odd q_i as it shown in Fig. 1 by dotted lines below the

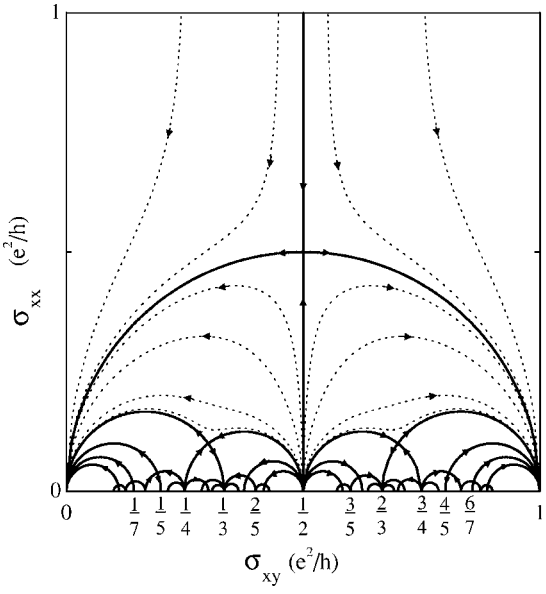

FIG. 1. The scaling flow diagram showing the coupled evolution of the diagonal (σ_{xx}) and Hall (σ_{xy}) conductivity components with increasing coherence length for a totally spin-polarized 2D electron system in the range $0 < \sigma_{xy} < 1$. Solid lines represent the semicircle separatrixes and dotted lines give examples of some other flow lines.

large semicircle separatrix of Eq. (2). For the sake of clarity, only a limiting number of semicircle separatixes having the larger diameters are shown. Since the flow lines do not intersect the separatrixes the latter divide the flow diagram into the regions where the flow lines can reach only particular points on the horizonal axis (i.e., particular QHE states).

As follows from the above consideration, the scaling theory[4–7] predicts the existence of a fractional quantum Hall effect (FQHE) at all rational fractions with odd denominators, including the recently observed[10] 4/11 and 5/13 states. To describe these states the widely accepted composite fermion picture[11] has to be modified by introducing the concept of higher generation composite fermions.[12–14]

According to the scaling theory,[5] close to zero temperature, transitions between QHE states occurring at variation of the magnetic field or the electron density are described by semicircles connecting corresponding points on the $(\sigma_{xy}, \sigma_{xx})$ diagram. Two such semicircles have been observed experimentally[15] for the case of transitions to the insulating state (0, 0) from the (1, 0) and from the (1/3, 0) QHE state.

It is worth noting that the flow lines depend on the magnetic field and such parameters of the system as electron density, disorder, or scattering mechanism only via the values of the magnetoconductances σ_{xy} and σ_{xx}. Where σ_{xy} is mainly determined by the electron density and the magnetic field, σ_{xx} is strongly dependent on the sample quality. For a better sample with higher mobility, the lower σ_{xx} value at given σ_{xy} and temperature allows the observation of a larger number of FQHE states. However, experimental limitations of attainable low temperatures do not allow us to reach the upper parts of the flow lines in the flow diagram for the high-mobility samples. Therefore, to investigate the total diagram, samples of very different quality should be utilized. The data presented here cover that part of the diagram, which corresponds to samples of moderate quality.

For the integer QHE, the experimentally obtained flow diagram[16] was in qualitative agreement with the theoretical picture. Quantitative agreement between theoretical[5] and experimental flow lines has been found for strongly disordered GaAs layers.[17] To the best of our knowledge the temperature driven flow diagram in the fractional QHE regime has been briefly investigated[18] for $1<\sigma_{xy}<2$ only. In this situation, the electron system is not fully spin polarized and the later appeared scaling theory[4] is not directly applicable. However, in a wide variety of samples,[19,20] for the transition from the fractional state (1/3, 0) to the insulating state (0, 0), the value of ρ_{xx} at the temperature independent point has been found to be close to the theoretical critical value $\rho_{xx}^{c}=h/e^2$.

In the work presented here we explore the temperature driven flow diagram of $\sigma_{xx}(T)$ versus $\sigma_{xy}(T)$ for a two-dimensional (2D) electron system in $GaAs/Al_xGa_{1-x}As$ heterostructures in the fractional QHE regime with $\sigma_{xy}<2/3$. A good agreement with the recent scaling theories is found, which implies surprisingly that at low enough temperatures the evolution with temperature of a totally spin-polarized 2D electron system depends only on initial values of σ_{xy} and σ_{xx} and that the behavior in different parts of the $(\sigma_{xy}, \sigma_{xx})$ plane is connected by simple transformations according to Eq. (1).

Two samples of molecular beam epitaxy (MBE) grown $GaAs/Al_{1-x}Ga_xAs$ heterostructures from different wafers were used in our experiments. They have an undoped $Al_{1-x}Ga_xAs$ spacer of 50 and 70 nm for samples 1 and 2, respectively. Sample 1, without gate structure, has a low-temperature electron density $n=1.35\times10^{11}$ cm^{-2} and a mobility 8.8×10^4 cm^2/Vs. Sample 2, with a gate structure, has an electron density $n=1.4\times10^{11}$ cm^{-2} and a mobility 1.2×10^6 cm^2/Vs at zero gate voltage. Previous study of sample 2 (Ref. 21) proved a spin-depolarization of the 2D electron system at filling factors $2/3<\nu<1$, in agreement with theoretical prediction.[22] For this reason we limit the here presented flow diagrams to $0<\sigma_{xy}<2/3$. Note that because of very different mobilities of these two samples the same values of σ_{xy} and σ_{xx} at the same temperature are obtained at very different electron densities. For example, the point (0.5,0.1) for sample 2 is reached at $n\approx3\times10^{10}$ cm^{-2}, a factor of 4 smaller than the carrier density in sample 1. The Hall bar geometry was used for measurements of the Hall (ρ_{xy}) and diagonal (ρ_{xx}) resistivities. For sample 1 without a gate the diagonal (ρ_{xx}) and Hall (ρ_{xy}) resistivities have been measured as a function of the magnetic field B at different temperatures and converted into the $\sigma_{xx}(B)$ and $\sigma_{xy}(B)$ data. For sample 2 with a gate ρ_{xx} and ρ_{xy} have been measured as a function of the gate voltage V_g at different temperatures for three fixed magnetic fields 2.5, 2.8, and 6 T. The absolute values of the Hall ρ_{xy} signals were appreciably different for two opposite directions of the magnetic field at the highest fields for sample 1 and the lowest gate voltages for sample 2, probably because of an admixture of ρ_{xx} to ρ_{xy}. The average has been taken as ρ_{xy}.

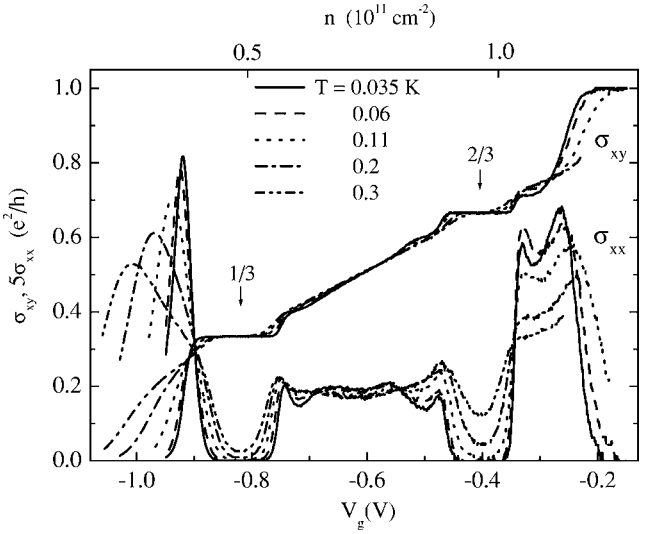

FIG. 2. The diagonal (σ_{xx}) and Hall (σ_{xy}) conductivities as a function of the gate voltage for sample two at a 6.0 T magnetic field for different temperatures below 0.3 K. The arrows indicate the gate voltage positions of the σ_{xx} minima for fractional QHE states 2/3 and 1/3.

The corresponding data for $\sigma_{xx}(V_g)$ and $\sigma_{xy}(V_g)$ (both given in units of e^2/h) are shown in Fig. 2 for $B=6$ T. The two fractional QHE states (2/3 and 1/3) are well pronounced especially at the lowest temperature. These well developed FQHE states are observed together with weakly pronounced 2/5 and 3/5 states. The upper axis for the electron

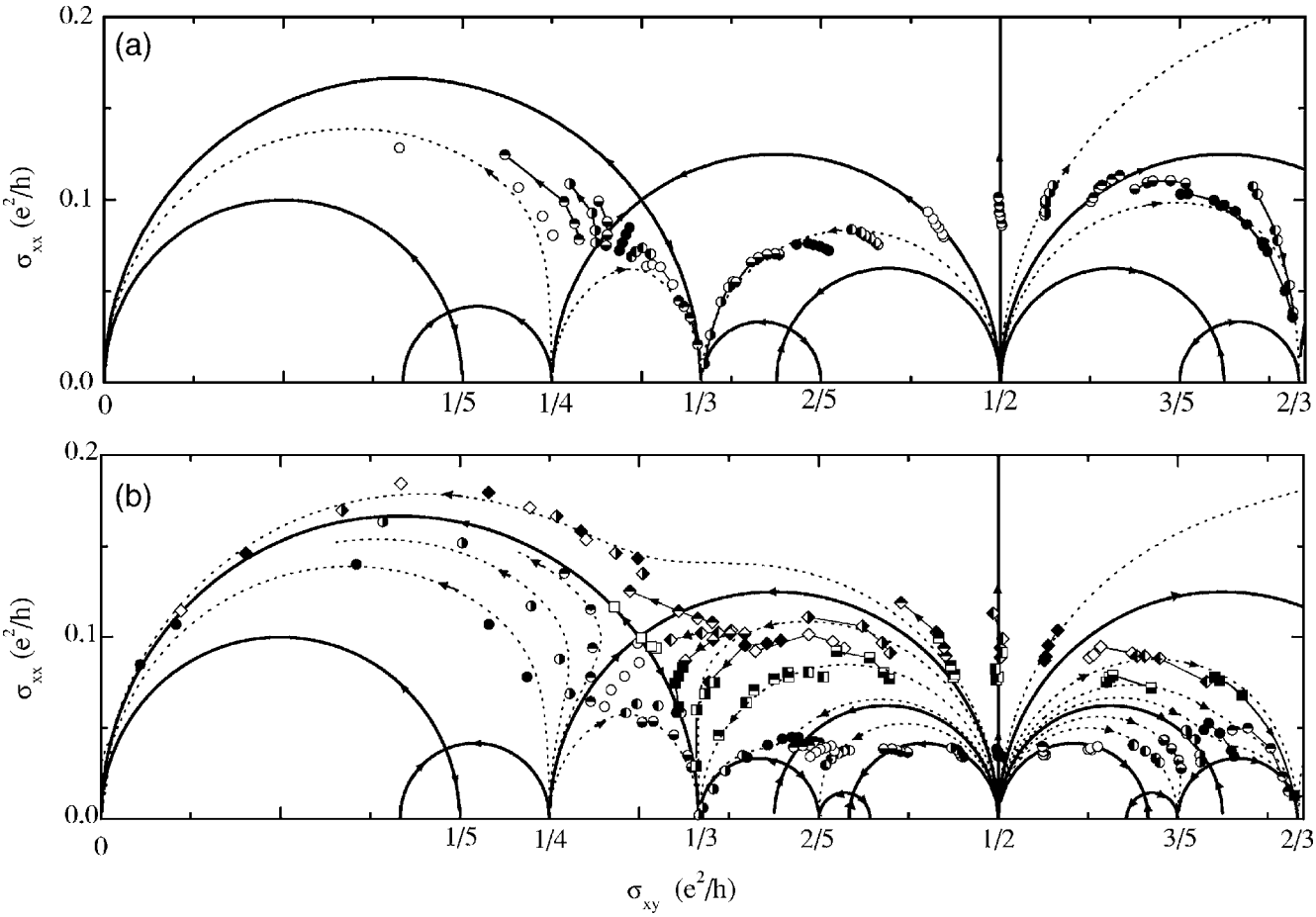

FIG. 3. The flow diagram of the temperature-dependent $[\sigma_{xy}(T), \sigma_{xx}(T)]$ data points (a) for sample 1 from 0.37 down to 0.05 K (for $1/3 < \sigma_{xy} < 2/3$) and down to 0.11 K (for $\sigma_{xy} < 1/3$) at different magnetic fields in the range 8.5–21 T, and (b) for sample two from 0.3 down to 0.035 K at different gate voltages for $B=2.5$ (diamonds), 2.8 (squares, a few data), and 6 T (circles). Different fillings of the symbols are used for different magnetic fields (data of sample 1) and for different gate voltages (data of sample 2). Solid lines represent the theoretical vertical and semicircle separatrixes. Dotted lines show flow lines close to experimental data.

density n is slightly nonlinear below $n \approx 3 \times 10^{10}$ cm^{-2}. An additional shallow minimum in σ_{xx} and a step in σ_{xy} can be seen at $n=1.1 \times 10^{11}$ cm^{-2} ($\nu \approx 0.75$). However, their evolution with temperature differs from the usual behavior for the fractional QHE. The value of σ_{xx} in the minimum increases with decreasing temperature and the plateau value of σ_{xy} depends on temperature. This observation is in agreement with earlier results[23] and probably originates from partial spin polarization of the 2D electron system at filling factors $2/3 < \nu < 1$ which makes the theory[4–8] inapplicable in this range. At $B=2.5$ and 2.8 T, the fractional QHE is observed only at $\nu=1/3$ and $2/3$ as for the data of sample 1.

In Fig. 3, the experimental flow data are compared with theoretical flow diagram and rather good agreement is demonstrated. For sample one [Fig. 3(a)] at $\sigma_{xy}=1/2$ the flow of the experimental data goes vertically up in accordance with the theory. To the left of this line the flow lines deviate to the left and are nearly horizontal around $\sigma_{xy}=0.4$, before curving down tending to (1/3, 0). Similarly to the right of $\sigma_{xy}=1/2$ the experimental flow deviates to the right, is almost horizontal around $\sigma_{xy}=0.6$, and then curves down tending to (2/3, 0). At $0.25 < \sigma_{xy} < 0.3$ the flow lines go approximately up at the beginning and diverge near the critical point close to the theoretically predicted one at (0.3, 0.1).

For sample 2 [Fig. 3(b)], the experimental points reproduce a large part of the theoretical flow lines connecting points (1/2, 0) and (1/3, 0); (1/2, 0) and (2/3, 0); (1/4, 0) and (0, 0), and follow vertical flow line at $\sigma_{xy}=1/2$. The flow line between the (1/2, 0) and (0, 0) points also demonstrate very good agreement with the experimental data. Note that the experimental points shift with lowering temperature always in the direction of the nearest flow lines in complete agreement with what is expected from the theory. For example, experimental points move with lowering temperature along the σ_{xx} axis upward in the vicinity of $\sigma_{xy}=1/2$ and $\sigma_{xy}=1/4$ and downward in the vicinity of $\sigma_{xy}=1/3$ and $\sigma_{xy}=2/3$. The theoretical flow lines directed to fractional QHE states with $\sigma_{xy}=2/5$ and $\sigma_{xy}=3/5$ are also rather well confirmed experimentally. A complicated picture exists in the vicinity of the theoretical critical point (0.3, 0.1). Corresponding data are shown in Fig. 4 on an enlarged scale. The experimental data can be well fitted by slightly deforming the separatrix connecting the (1/2, 0) and (1/4, 0) points (dotted line) as is shown by dash-dotted line in Fig. 4. The flow of the experimental data has a nontrivial character: the data points shift towards the critical point when located in

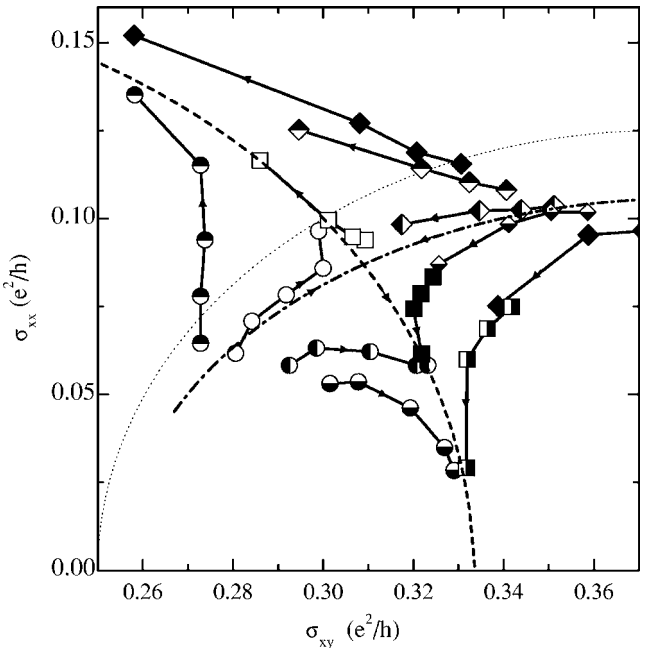

FIG. 4. A part of the flow diagram of Fig. 3(b) in the vicinity of the theoretical critical point (0.3, 0.1). Experimental points (diamonds for $B=2.5$, squares for 2.8, and circles for 6 T) are connected by solid lines and the direction of their shift with lowering temperature are shown by arrows. The theoretical semicircle separatrixes are presented by dashed and dotted lines. The dash-dotted line is obtained by a slight deformation of the dotted theoretical line.

the vicinity of the deformed separatrix and away from the critical point along separatrix connecting (1/3, 0) and (0, 0) points (dashed line). The separatrix deformation results in shift of the critical point to the (0.09, 0.31) position. Thus, there is only rather small quantitative discrepancy (about 10%) between theoretical and our experimental flow lines. This difference could be attributed to macroscopic inhomogeneity of the sample bearing in mind the data scattering for ρ_{xx}^{c}, 30% in Ref. 19 and 10% in Ref. 20.

The possible role of dissipationless edge currents could have an influence on the correct measurement of the magnetotransport tensor components in our experiment. The edge currents can shortcircuit the dissipative bulk conductivity so that neither magnetoresistivity nor magnetoconductivity can be determined from the measured magnetoresistance.[24,25] The shortcircuiting by edge currents could occur only at filling factors above a very well pronounced QHE state (or, equivalently, at magnetic fields and gate voltages, respectively, below and above QHE plateaux) giving rise to an asymmetric form of the magnetoconductivity $\sigma_{xx}(B)$ around a QHE minimum. Moreover, in the case of fractional QHE, edge currents exist only in a rather close vicinity of the corresponding QHE states[26] (for example, edge currents related to FQHE do not affect the conductivity at $\nu=1/2$). Considering our data below $\nu=2/3$, pronounced fractional QHE states occur only at $\nu=1/3$ at the lowest temperatures and highest fields with σ_{xx} approaching zero. Therefore, the data points on the flow lines converging to the insulating state (0, 0), those in the vicinity of the discussed critical point (0.09, 0.31), and those around and above $\sigma_{xy}=1/2$ up to 2/3 cannot be affected by the edge currents. The quite symmetric form of the magnetoconductivity minima at $\nu=1/3$ observed in our experiment even at the lowest temperatures (see Fig. 2 as an example) gives a further indication that edge currents aren't of importance in our data.

The theoretical flow diagram describes the behavior of a 2D system when only the coherence length depends on temperature with all other parameters being temperature independent. Such regime is obviously limited from both low and high temperature sides. At high temperatures, for example, the formation of an energy gap in the excitation spectrum with decreasing temperature is not included in the scaling theory. At low temperatures the transition to variable-range hopping could break the scaling description. However, the latter would change the flow diagram only in very close vicinity of the quantum Hall states. An estimation of the upper temperature limit for the scaling approach is not well established. Existing experimental results on the temperature dependence of the compressibility of a 2D electron system in the fractional quantum Hall effect regime[27,28] and on the nonmonotonic temperature dependence of σ_{xx} at $\sigma_{xy}=1/2$[29] imply the upper temperature limit for the scaling flow lines to be at approximately 0.5 K. In our samples at temperatures above 0.4 K the deviations of the experimental data from the scaling theory predictions increase gradually, consistently with results of Refs. 27–29.

In summary, for the fractional quantum Hall effect regime at $0<\sigma_{xy}<2/3$ we have found that the complicated temperature dependence of the magnetoconductivity tensor components when presented in the form of the flow lines on the $(\sigma_{xy},\sigma_{xx})$ plane is rather well quantitatively described by equations of the scaling theory.[4–7] The evolution of $(\sigma_{xy},\sigma_{xx})$ with decreasing temperature is determined uniquely by the initial values of σ_{xy} and σ_{xx} independently from the microscopic parameters of a totally spin-polarized 2D electron system.

The authors greatly appreciate producing of samples by MBE groups from Institute of Semiconductor Physics RAS, Novosibirsk, Russia (sample 1) and from Max-Planck-Institut für Festkörperforschung, Stuttgart, Germany (sample 2). This work was supported by the Russian Foundation for Basic Research.

[1] H. Levine, S. B. Libby, and A. M. M. Pruisken, Phys. Rev. Lett. **51**, 1915 (1983).
[2] D. E. Khmel'nitskiĭ, Pis'ma Zh. Eksp. Teor. Fiz. **38**, 454 (1983) [JETP Lett. **38**, 552 (1983)].
[3] A. M. M. Pruisken, in *The Quantum Hall Effect*, edited by R. E. Prange and S. M. Girven (Springer-Verlag, Berlin, 1990).
[4] C. A. Lütken and G. G. Ross, Phys. Rev. B **45**, 11837 (1992); **48**, 2500 (1993).
[5] B. P. Dolan, Nucl. Phys. B **554**, 487 (1999); J. Phys. A **32**, L243 (1999).
[6] C. P. Burgess, Rim Dib, and B. P. Dolan, Phys. Rev. B **62**, 15359 (2000).
[7] C. P. Burgess and B. P. Dolan, Phys. Rev. B **63**, 155309 (2001).
[8] A. M. M. Pruisken, M. A. Baranov, and B. Škorić, Phys. Rev. B **60**, 16807 (1999).
[9] S. Kivelson, D. Lee, and S. Zang, Phys. Rev. B **46**, 2223 (1992).
[10] W. Pan, H. L. Stormer, D. C. Tsui, L. N. Pfeiffer, K. W. Baldwin, and K. W. West, Int. J. Mod. Phys. B **16**, 2940 (2002); Phys. Rev. Lett. **90**, 016801 (2003).
[11] J. K. Jain, Phys. Rev. Lett. **63**, 199 (1989).
[12] C.-C Chang and J. K. Jain, Phys. Rev. Lett. **92**, 196806 (2004).
[13] Ana Lopez and Eduardo Fradkin, Phys. Rev. B **69**, 155322 (2004).
[14] M. O. Goerbig, P. Lederer, and C. Morais Smith, Phys. Rev. B **69**, 155324 (2004); Europhys. Lett. **68**, 72 (2004).
[15] M. Hilke, D. Shahar, S. H. Song, D. C. Tsui, Y. H. Xie, and M. Shayegan, Europhys. Lett. **46**, 775 (1999).
[16] H. P. Wei, D. C. Tsui, and A. M. M. Pruisken, Phys. Rev. B **33**, 1488 (1986).
[17] S. S. Murzin, M. Weiss, A. G. M. Jansen, and K. Eberl, Phys. Rev. B **66**, 233314 (2002).
[18] R. G. Clark, J. R. Mallett, A. Usher, A. M. Suckling, R. J. Nicholas, S. R. Haynes, and Y. Journaux, Surf. Sci. **196**, 219 (1988).
[19] D. Shahar, D. C. Tsui, M. Shayegan, R. N. Bhatt, and J. E. Cunningham, Phys. Rev. Lett. **74**, 4511 (1995).
[20] L. W. Wong, H. W. Jiang, N. Trivedi, and E. Palm, Phys. Rev. B **51**, 18033 (1995).
[21] S. I. Dorozhkin, M. O. Dorokhova, R. J. Haug, and K. Ploog, Phys. Rev. B **55**, 4089 (1997).
[22] T. Chakraborty, Surf. Sci. **229**, 16 (1990).
[23] R. J. Haug, K. v. Klitzing, R. J. Nicholas, J. C. Maan, and G. Weimann, Phys. Rev. B **36**, 4528 (1987).
[24] B. E. Kane, D. C. Tsui, and G. Weimann, Phys. Rev. Lett. **59**, 1353 (1987).
[25] S. I. Dorozhkin, S. Koch, K. von Klitzing, and G. Dorda, Pis'ma Zh. Eksp. Teor. Fiz. **52**, 1233 (1990) [JETP Lett. **52**, 652 (1990)].
[26] J. K. Wang and V. J. Goldman, Phys. Rev. Lett. **67**, 749 (1991); Phys. Rev. B **45**, 13479 (1992).
[27] S. I Dorozhkin, G. V. Kravchenko, R. I. Haug, K. von Klitzing, and K. Ploog, Pis'ma Zh. Eksp. Teor. Fiz. **58**, 893 (1993) [JETP Lett. **58**, 834 (1994)].
[28] J. P. Eisenstein, L. N. Pfeiffer, and K. W. West, Phys. Rev. B **50**, 1760 (1994).
[29] L. P. Rokhinson, B. Su, and V. J. Goldman, Phys. Rev. B **52**, 11588 (1995).